



Accurate bacterial outbreak tracing with Oxford Nanopore sequencing and reduction of methylation-induced errors

Mara Lohde, Gabriel E. Wagner, Johanna Dabernig-Heinz, et al.

Genome Res. 2024 34: 2039-2047 originally published online October 23, 2024

Access the most recent version at doi:[10.1101/gr.278848.123](https://doi.org/10.1101/gr.278848.123)

References This article cites 44 articles, 4 of which can be accessed free at:
<http://genome.cshlp.org/content/34/11/2039.full.html#ref-list-1>

Open Access Freely available online through the *Genome Research* Open Access option.

Creative Commons License This article, published in *Genome Research*, is available under a Creative Commons License (Attribution 4.0 International), as described at <http://creativecommons.org/licenses/by/4.0/>.

Email Alerting Service Receive free email alerts when new articles cite this article - sign up in the box at the top right corner of the article or [click here](#).



To subscribe to *Genome Research* go to:
<https://genome.cshlp.org/subscriptions>

© 2024 Lohde et al.; Published by Cold Spring Harbor Laboratory Press

Method

Accurate bacterial outbreak tracing with Oxford Nanopore sequencing and reduction of methylation-induced errors

Mara Lohde,¹ Gabriel E. Wagner,² Johanna Dabernig-Heinz,² Adrian Viehweger,³ Sascha D. Braun,^{4,5} Stefan Monecke,^{4,5} Celia Diezel,^{4,5} Claudia Stein,¹ Mike Marquet,¹ Ralf Ehricht,^{4,5,6} Mathias W. Pletz,^{1,4} and Christian Brandt^{1,4}

¹Institute for Infectious Diseases and Infection Control, Jena University Hospital, 07747 Jena, Germany; ²Diagnostic and Research Institute of Hygiene, Microbiology and Environmental Medicine, Medical University of Graz, 8010 Graz, Austria; ³Institute of Medical Microbiology and Virology, University Hospital Leipzig, 04103 Leipzig, Germany; ⁴InfectoGnostics Research Campus, Center for Applied Research, 07743 Jena, Germany; ⁵Leibniz-Institute of Photonic Technology (Leibniz-IPHT), 07745 Jena, Germany; ⁶Institute of Physical Chemistry, Friedrich-Schiller-University Jena, 07743 Jena, Germany

Our study investigates the effectiveness of Oxford Nanopore Technologies for accurate outbreak tracing by resequencing 33 isolates of a 3-year-long *Klebsiella pneumoniae* outbreak with Illumina short-read sequencing data as the point of reference. We detect considerable base errors through cgMLST and phylogenetic analysis of genomes sequenced with Oxford Nanopore Technologies, leading to the false exclusion of some outbreak-related strains from the outbreak cluster. Nearby methylation sites cause these errors and can also be found in other species besides *K. pneumoniae*. Based on these data, we explore PCR-based sequencing and a masking strategy, which both successfully address these inaccuracies and ensure accurate outbreak tracing. We offer our masking strategy as a bioinformatic workflow (MPOA) to identify and mask problematic genome positions in a reference-free manner. Our research highlights limitations in using Oxford Nanopore Technologies for sequencing prokaryotic organisms, especially for investigating outbreaks. For time-critical projects that cannot wait for further technological developments by Oxford Nanopore Technologies, our study recommends either using PCR-based sequencing or using our provided bioinformatic workflow. We advise that read mapping-based quality control of genomes should be provided when publishing results.

[Supplemental material is available for this article.]

Whole-genome sequencing is essential for analyzing outbreaks, pandemics, or phylogenetic relationships (Chewapreecha et al. 2017; Wyres et al. 2020). The recent SARS-CoV-2 pandemic has thus led to a leap in the integration and expansion of sequencing capacities in many laboratories and hospitals, predominantly using Illumina for short-read sequencing or Oxford Nanopore Technologies (ONT) for long-read sequencing (~78% and 18%, respectively) (Brandt et al. 2021). Beyond viral pandemic tracking, bacterial pathogen outbreaks, particularly those linked to antibiotic resistance, continue to impose a significant global public health burden (Murray et al. 2022). Gram-negative bacteria, in particular, rapidly acquire antibiotic resistance via horizontal gene transfer from other species (Lerminiaux and Cameron 2019; Hadjadj et al. 2022; Moura de Sousa et al. 2023). This mechanism complicates tracking outbreaks or identifying their origin, as a single specific plasmid or mobile element can be responsible for a persistent outbreak or multiple outbreaks across unrelated species (Sivertsen et al. 2014; Pletz et al. 2018; Abe et al. 2021; Hadjadj et al. 2022). Additionally, in Gram-negative bacteria, DNA methylation plays a crucial role in epigenetic regulation, which impacts gene expres-

sion, genome modification, virulence, mismatch repair, and other physiological activities (Gao et al. 2023; Wang et al. 2023).

Effectively tracking these complex molecular mechanisms requires careful strategic monitoring and sequencing-based investigation. Consequently, the accuracy and continuity of the genome data are paramount. Illumina, a short-read sequencing method with an error rate of <0.8% in raw data, is frequently used as its complementary genome reconstruction precision exceeds 99.997% (Wang et al. 2021). However, repetitive elements, such as transposons, present a substantial challenge for short reads when reconstructing closed bacterial genomes and their accompanying plasmids. Long-read sequencing technologies like Pacific Biosciences (PacBio) and ONT can resolve such elements, for example, plasmids, as they achieve longer read lengths averaging ~10–20 kb and even up to 3.85 Mb in the case of ONT (Eid et al. 2009; Grohme et al. 2018; Tyson et al. 2018; Dohm et al. 2020).

Real-time sequencing allows data collection and analysis, whereas sequencing positions ONT as an appealing choice for hospital surveillance and outbreak control (Spott et al. 2022). Owing to their recently launched flow cells (R10.4.1) and chemistry (SQK-NBD114.24), they have achieved raw read accuracy that now exceeds 99.1% (Ni et al. 2023). Several studies have shared their findings and reported accuracy levels similar to those from

Corresponding author: mara.lohde@med.uni-jena.de

Article published online before print. Article, supplemental material, and publication date are at <https://www.genome.org/cgi/doi/10.1101/gr.278848.123>. Freely available online through the *Genome Research* Open Access option.

© 2024 Lohde et al. This article, published in *Genome Research*, is available under a Creative Commons License (Attribution 4.0 International), as described at <http://creativecommons.org/licenses/by/4.0/>.

short-read data (Sanderson et al. 2023; Wagner et al. 2023). However, significant discrepancies between Illumina and ONT genomes were also observed for some organisms (Linde et al. 2023).

These contradictions can lead to inaccurate conclusions, like excluding outbreak-associated samples when investigating outbreaks. In addition, genomes are usually stored in open public databases such as NCBI or ENA, which can lead to error propagation and can potentially significantly affect patients' welfare. Therefore, we used ONT to reevaluate a well-documented, 3-year-long outbreak initially analyzed with Illumina data to address these contradictory statements, focusing on the errors in ONT sequencing data (Viehweger et al. 2021). *Klebsiella pneumoniae* is an ideal microorganism for this topic, as it is a common pathogen linked to hospital-wide outbreaks carrying plasmids with multi-drug-resistance genes (Brandt et al. 2019). When using ONT-only data, we identified a few critical issues leading to erroneous basecalls for *K. pneumoniae*. We noticed similar problems and clear patterns in other organisms, which need to be considered during outbreak identification, even though we could resolve them.

Results

Erroneous basecalls occur in some strains but not others and vary by basecaller and sequencing kits

We resequenced the genomes of 33 randomly distributed *K. pneumoniae* samples isolated from 31 patients (from a total of 114 outbreak-related isolates) using R10.4 and R10.4.1 flow cells, along with the corresponding library preparation kits (henceforth "Kit 12": SQK-NBD112.24 [early access] and "Kit 14": SQK-NBD114.24 [successor]). Our objective was to investigate whether previously reported conflicting statements could be replicated (Linde et al. 2023; Sanderson et al. 2023; Wagner et al. 2023). We used core genome multilocus sequence typing (cgMLST) to compare ONT and Illumina-sequenced genomes. The comparison of the 33 samples revealed 11 outliers in the ONT data, showing high allelic deviations (up to 46) to their short-read counterparts while not matching the outbreak cluster (Supplemental Figs. 1 and 2). Although the remaining samples closely match the outbreak cluster, the outliers highlight inconsistencies within the ONT data, as reported in the literature. To assess whether either

the basecaller or their models might be responsible, we rebasecalled and compared an outlier sample (UR2602) in detail to three samples, for which we assume error-free genomes based on cgMLST (for further details, see subsection "Basecalling and assembly" in the Methods) (Fig. 1) and pairwise SNP calling (Supplemental Fig. 3) with Illumina genomes.

Based on 2358 loci for the cgMLST, no allelic differences, regardless of kit, basecaller, or basecaller model, were identified for the isolates UR14350, VA13324, and TP3419. In contrast, the outlier sample (UR2602) revealed allelic variations for each kit, basecaller, and sequencing technology. Despite both basecallers using the same raw signal data, the 35 allelic variations in Guppy differ without accordance from the 44 allelic variations in Dorado.

By cgMLST, the outlier sample prepared with Kit 14 would be falsely assigned as not part of the outbreak owing to its 35 or 44 allelic differences, even though the sample exhibits low allelic differences according to the short-read data (gold standard). Conversely, when prepared with early access Kit 12, the same isolate would be correctly considered as only four different loci could be observed (adhering to the recommended allelic difference cutoff of 15 or less) (Miro et al. 2020). Because the basecalling models disagreed on the allelic differences, we suspected more issues within the raw data (reads and raw signals) and conducted a comprehensive analysis of all possible affected positions.

Ambiguities in purine or pyrimidine discrimination for a subset of genome positions can cause erroneous basecalls

The first visual inspection of mapped reads to the assembly revealed read ambiguity on certain positions indicated by varying base ratios (ambiguous positions). For further characterization of these ambiguous positions, we examined our data at the sequence, nucleotide, and raw signal level (Fig. 2). For each ambiguous position on the chromosomal DNA for 33 *K. pneumoniae* outbreak samples, we determined the ratio between the two bases by counting their occurrences for both strand orientations within the read data at that position (Fig. 2A). Searching for characteristic "indicator" sequence motifs, we explored the surrounding base for each detected ambiguous position and plotted the observed pattern as a sequence logo (Fig. 2B; Supplemental Table 1). Additionally, we

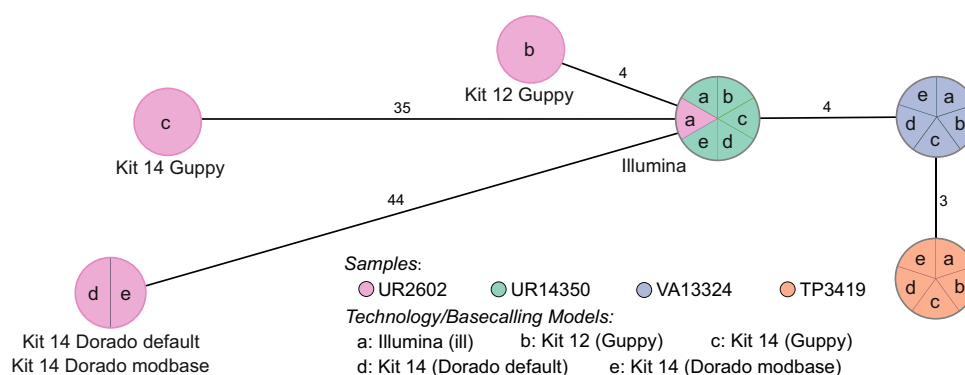


Figure 1. cgMLST typing reveals allelic differences between genomes utilizing different basecaller models and sequencing kits. The minimum spanning tree pictures four *K. pneumoniae* samples based on 2358 genes for pairwise comparison of allelic variations. Missing values were ignored. Nodes (samples) are connected by lines depicting the distance by numbers of allelic differences. Loci are considered different if one or more bases change between the samples. Loci without allelic differences are described as being the same. Samples with allelic differences of 15 or fewer are considered as part of the cluster. All isolates were prepared with Kit 14 and Kit 12 and basecalled with each respective Guppy "superaccurate" basecalling model (see subsection "Basecalling and assembly" in the Methods). We basecalled all Kit 14–prepared samples with Dorado using the default and a modification-aware model (see subsection "Basecalling and assembly" in the Methods).

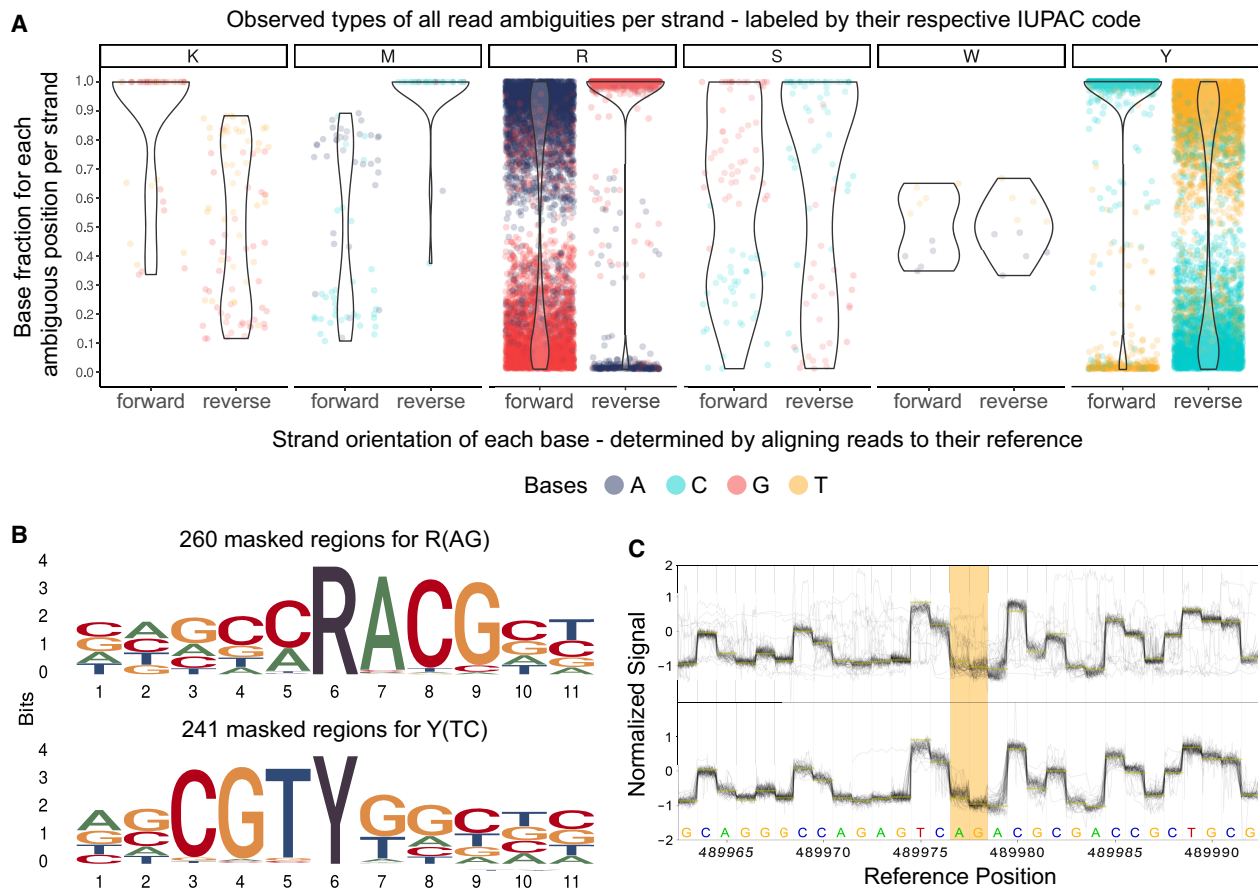


Figure 2. Systematic examination of ambiguous positions for frequency by strand orientation (A), conserved sequences (B), and raw Nanopore signal (C). (A) Violin chart showing the ratio between two bases within the mapped read data separated by strand orientation for 6556 ambiguous positions in 33 *K. pneumoniae* samples. Every ambiguous position is divided by which two bases appear and is labeled by their respective degenerative base (IUPAC nucleotide code). For example, “R” stands for a combination in which either A or G is found at that position. Each dot represents a base occurrence within the respective base combination at the ambiguous position. (B) Sequence logo of observed sequence pattern around the ambiguous bases R and Y on the chromosomal contig of *K. pneumoniae* for one sample. (C) Raw signal level (FAST5/PODS) of ambiguous positions (yellow) for Kit 14 (above) with methylated bases and SQK-RPB114.24 without modifications (below). Less clear signals are observable in ambiguous positions (yellow) for Kit 14. Signal plots were generated with remora (v.2.1.3; <https://github.com/nanoporetech/remora>).

compared the methylated and unmethylated raw signals around these ambiguous positions (Fig. 2C).

As highlighted in Figure 2A, in some positions, the basecaller cannot determine between either of two bases, expressed by specific base ratios varying per position and strand orientation, resulting in erroneous assemblies. We could not observe ambiguous positions containing more than two different bases. For clarity, we assign the IUPAC nucleotide code for degenerate bases (R, Y, M, K, S, W) to each ambiguous position varying between two bases. Accordingly, we will refer, for example, to “R” when the positions contain A or G in the read data.

Out of our analysis of 33 *K. pneumoniae* outbreak isolates, we discovered 6556 positions that exhibit ambiguity (Fig. 2A). The ambiguity mainly resolved around 3311 positions for R and 3111 for Y. In 5442 of 6455 R and Y positions (84.31%), the basecalled reads lean toward cytosine or guanine (C or G). We detected other ambiguous positions in K (44), M (34), S (51), and W (5), but with comparable lower occurrences. It is essential to acknowledge that not all identified ambiguous positions result in errors in the assembled genome, which explains the varying error profile of the same sample (Fig. 1). Errors in these ambiguous positions mainly arise when de-

terminating between purine bases (A or G) or pyrimidine bases (T or C). Because strand bias is reported as a substantial factor for false-positive variant detection, we considered the strand orientation of the read data (Leija-Salazar et al. 2019). In most cases, we noticed that the correct base is located clearly and more frequently on both strand orientations, whereas the incorrect base is less prevalent. For instance, the correct base guanine is found on both strands for positions masked by R and is predominantly found on the reverse strand (Fig. 2A, see R reverse) and less frequently on the forward strand, which also contains the false base. We detected similar behavior for other species (Supplemental Fig. 6).

In the error-prone genomes of the *K. pneumoniae* outbreak, we detected preserved patterns around the ambiguous positions R and Y (Fig. 2B). These sequence motifs are reverse-complement patterns (RACG/CGTY), pointing to a singular issue. We also observed additional patterns compared with other isolates of *K. pneumoniae*. These motifs are likely specific to particular strains.

Furthermore, we examined and collected additional ONT sequencing data that used the Kit 14 library preparation (264 isolates across 32 species) to investigate whether the ambiguous positions are *K. pneumoniae* exclusive (Table 1). These samples were collected

Table 1. Overview of R (A–G) and Y (T–C) base ambiguity for 264 isolates from 32 species, sequenced with Oxford Nanopore Technologies using Kit 14

Species	Total samples	Samples with >50 ambig. P	Mean R (A–G) ambiguity per sample (min/max)	Mean Y (T–C) ambiguity per sample (min/max)	Motif type	Reference
<i>Achromobacter xylosoxidans</i>	1	0 (0%)	6	4	NA	^a
<i>Acinetobacter baumannii</i>	15	5 (33.33%)	22.53 (0/109)	19.87 (0/83)	NA	^a
<i>Acinetobacter junii</i>	1	1 (100%)	279	223	CARATG CATYTG	^a
<i>Acinetobacter mesopotamicus</i>	1	1 (100%)	53	28	NA	^a
<i>Acinetobacter radioresistens</i>	1	1 (100%)	175	150	RA TY	^a
<i>Acinetobacter soli</i>	1	0 (0%)	12	11	NA	^a
<i>Bordetella pertussis</i> ^d	40	0 (0%)	0.1 (0/1)	0.2 (0/1)	NA	(Wagner et al. 2023)
<i>Chryseobacterium arthrophaerae</i>	1	0 (0%)	13	7	NA	^a
<i>Chryseobacterium gleum</i>	1	1 (100%)	218	217	RACGC GCGTY	^a
<i>Citrobacter freundii</i>	3	3 (100%)	145.67 (49/329)	137.67 (39/319)	CRATGTC GACATYG	^a
<i>Citrobacter portucalensis</i>	2	2 (100%)	29 (26/32)	29 (28/30)	RA TY	^a
<i>Enterobacter cloacae</i>	1	1 (100%)	153	162	NA	^a
<i>Enterobacter hormaechei</i>	5	1 (20%)	15.60 (4/45)	15.60 (6/42)	NA	^a
<i>Enterococcus faecalis</i>	10	10 (100%)	250.40 (223/275)	249.00 (210/270)	TRAG CTYA	^c
<i>Enterococcus faecium</i>	19	2 (10.53%)	15.74 (0/27)	14.63 (0/28)	RACC GGTY	(Dabernig-Heinz et al. 2024) ^b
<i>Escherichia coli</i>	8	3 (37.50%)	31.38 (2/118)	29.31 (4/111)	NA	^a
<i>Escherichia flexneri</i>	10	9 (90%)	49.10 (19/88)	44.70 (18/88)	RAT ATY	^a
<i>Klebsiella aerogenes</i>	1	0 (0%)	22	17	NA	^a
<i>Klebsiella michiganensis</i>	1	1 (100%)	56	42	NA	^a
<i>Klebsiella pneumoniae</i>	70	38 (54.29%)	97.04 (3/835)	92.47 (3/847)	RACG CGTY	(Viehweger et al. 2021) ^{a,b}
<i>Klebsiella oxytoca</i>	1	0 (0%)	5	9	NA	^a
<i>Listeria monocytogenes</i>	17	3 (17.65%)	37.94 (0/514)	40.82 (0/557)	NA	^b
<i>Micrococcus luteus</i>	1	1 (100%)	172	220	CRAC GTYG	^a
<i>Proteus mirabilis</i>	1	1 (100%)	45	43	CRAC GTYG	^a
<i>Pseudomonas aeruginosa</i>	19	6 (33.33%)	389.17 (0/2251)	387.56 (0/2290)	AARACC GGTYTT	^a
<i>Pseudomonas asiatica</i>	2	1 (50%)	145 (0/290)	144.50 (0/289)	CCRA TYGG	^a
<i>Pseudomonas stutzeri</i>	1	0 (0%)	14	16	NA	^a
<i>Salmonella enterica</i>	2	1 (50%)	41.5 (7/76)	42.5 (7/78)	NA	^a
<i>Stenotrophomonas maltophilia</i>	1	1 (100%)	229	171	TAC RAC GT YGTA	^a
<i>Serratia marcescens</i>	4	4 (100%)	107.75 (68/178)	99.5 (67/171)	CCRA TYGG	^a
<i>Shewanella algae</i>	2	2 (100%)	71.5 (37/106)	50 (32/68)	NA	^a
<i>Staphylococcus aureus</i>	20	8 (40%)	23.35 (0/99)	23.35 (0/97)	RACC GGTY	^b

Only chromosomal contigs were analyzed, and only “superaccurate” basecalling models were used. Chromosomes were coverage-masked by N if below a read depth of 10x. N positions were not considered for the table to avoid overestimating one base ambiguity.

^aSequenced strains received from Leibniz-Institute of Photonic Technology, Optisch-Molekulare Diagnostik und Systemtechnologie.

^bSequenced strains received from Diagnostic and Research Institute of Hygiene, Microbiology and Environmental Medicine, Medical University of Graz.

^cOwn samples from the Jena University Hospital.

^dSequenced with Kit 12; resequencing via Kit 14 showed no differences.

based solely on Kit 14 library preparations and not on whether they were associated with an outbreak. We determine, compared to all other species samples, the fewest ambiguous positions (zero to one) in *Bordetella pertussis*. In contrast, all 10 *Enterococcus faecalis* isolates had more than 200 ambiguous positions. More than 40% of 264 screened samples have more than 50 ambiguous positions. Across all species, the minimal shared sequence motif was RA/TY. Certain species, such as *Acinetobacter junii*, *Acinetobacter radioresistens*, *Chryseobacterium gleum*, *Enterobacter cloacae*, *Micrococcus luteus*, and *Stenotrophomonas maltophilia*, exhibited a considerable number of ambiguous positions. This suggests that many species may be impacted, but not necessarily all strains.

As methylated bases are probably liable for ambiguous positions, we compared sequencing data with methylations (Kit 14) (Fig. 2C, above) and without (SQK-RPB114.24) (Fig. 2C, below) on the raw signal level from FAST5/POD5 files before basecalling occurs. We choose the raw signal level for investigation prior to any bioinformatic approaches (e.g., basecalling, assembly, polishing) to avoid the potential introduction of other biases or errors. For native sequencing, less clear signals at these positions are observable, which might cause these ambiguous basecalls. These noisy signals could explain the frequencies of bases we detected in the reads (Fig. 2A) and, thus, the basecaller's difficulty in deciding on a specific base for that position.

We found no coherent methylation motifs in the literature that would fit the observed pattern. Nevertheless, it has been reported that methylated bases can affect the raw signal in the surrounding region (Tourancheau et al. 2021). Thus, we cannot determine whether multiple methylation motifs are the cause or whether an unknown motif is present. Accordingly, to these findings, we evaluated whether PCR-based sequencing or a bioinformatic masking strategy for ambiguous positions can reliably remove these methylation-based errors for outbreak analysis.

Strategies to mitigate methylation-induced basecalling errors

To solve methylation-induced basecalling errors in ambiguous base positions, we evaluated two strategies: (1) We resequenced 10 *K. pneumoniae* outbreak samples using the Nanopore rapid PCR barcoding kit (SQK-RPB114.24) to remove methylated bases prior to sequencing and analyzed the genomes using cgMLST and phylogenetic analysis (Fig. 3A,B), and (2) we masked ambiguous positions for Kit 14 prepared genomes with our bioinformatic workflow (see subsection "Workflow for detection and masking of ambiguous positions" in the Methods). It is important to mention that these masked assemblies cannot be used for cgMLST because allelic differences cannot be accurately determined for genes with masked bases. Therefore, the masked genomes were only used for phylogenetic analysis (Fig. 3B). Furthermore, it should be noted that cgMLST only considers coding sequences, whereas the phylogenetic analysis assesses the entire genome that is represented in all samples, which gives a higher resolution for base differences.

When comparing the native barcoding with the PCR-based kit, ambiguous positions were significantly reduced from 2357 to just 44 for R and Y across the 10 resequenced *K. pneumoniae* samples (Supplemental Table 2). Both the minimum spanning trees and the phylogenetic tree also show this significant improvement in genome quality for ONT (Fig. 3). According to the cgMLST, the outlier samples UR2602 and BK12739 now closely match the Illumina genome, down to only one allele difference, from 35/33 (Fig. 3A). When comparing phylogenetic distances within the phylogenetic tree, an increased convergence with the Illumina ge-

nomes, particularly for the outlier samples, was observed, too (Fig. 3B). Additionally, masked and PCR-based assemblies have almost no phylogenetic divergence.

Further, we analyzed the phylogenetic tree containing native Kit 14, masked native Kit 14, and Illumina genomes for all 33 *K. pneumoniae* samples (Supplemental Fig. 4). These include 11 Kit 14 outliers (average of 492 ambiguous positions) and 22 Kit 14 genomes with an average of less than 52 ambiguous positions. We observed two types of phylogenetic distances between ONT Kit 14 and Illumina: The expected considerable distances between the outlier and Illumina genomes are because of ambiguity and, in some cases, a phylogenetic distance for which ambiguity is not the causation.

By masking ambiguous bases, we observed that eight of 11 outlier genomes now closely align with their respective Illumina genome. The remaining three outlier samples changed their tree positions after masking, now closely aligned with other Illumina genomes but still diverged from their corresponding Illumina genome owing to other non-ambiguity-related differences. For the other 22 masked Kit 14 genomes with less ambiguity than the outliers, we did not observe any substantial changes in their tree positions, as fewer positions were masked.

In summary, 22 out of 33 masked ONT genomes align with their respective Illumina genomes, and the remaining 11 do not. In these cases, the remaining distances do not result from ambiguous positions within the ONT assemblies. For instance, the Illumina and ONT genomes of TP3870 matched perfectly in the minimum spanning tree, but they exhibited some distance from each other in the phylogenetic tree (Supplemental Fig. 4). We identified reconstruction issues in these short-read assemblies, primarily manifesting in noncoding regions (Supplemental Fig. 5). Because cgMLST only compares coding sequences, these errors do not affect the result analysis. Therefore, we recommend using only one technology when performing whole-genome comparison for outbreak analysis.

Discussion

Over the past few years, ONT has been effectively used to monitor and track the SARS-CoV-2 pandemic and its viral lineages. Despite this, contradictory reports have emerged regarding the consistency of ONT-sequenced bacterial genomes compared with those that are Illumina based. Our research examined whether ONT can be used to analyze bacterial outbreaks accurately.

For our investigation, we resequenced a well-documented, 3-year-long *K. pneumoniae* outbreak using the Nanopore native barcoding Kit 14 for library preparation. Our analyses demonstrated that the raw signals were impacted by methylated bases, creating ambiguous positions through basecalling and leading to erroneous exclusions of certain outbreak-associated strains. However, not all isolates are affected by these ambiguities, and none or minimal allelic differences are shown in the corresponding short-read data. One should note that some errors in noncoding areas for Illumina assemblies were observed, which can lead to higher distances within a phylogenetic tree but with little to no effect in cgMLST. Despite focusing on *K. pneumoniae* initially, other prokaryotic organisms are also impacted. Crucially, we also detected ambiguous positions using the predecessor sequencing kit SQK-LSK109 (Supplemental Table 3). Consequently, when using ONT-based sequence data from open public databases or when analyzing outbreaks, one should test for read ambiguity by using, for example, the provided MPOA workflow before further analysis.

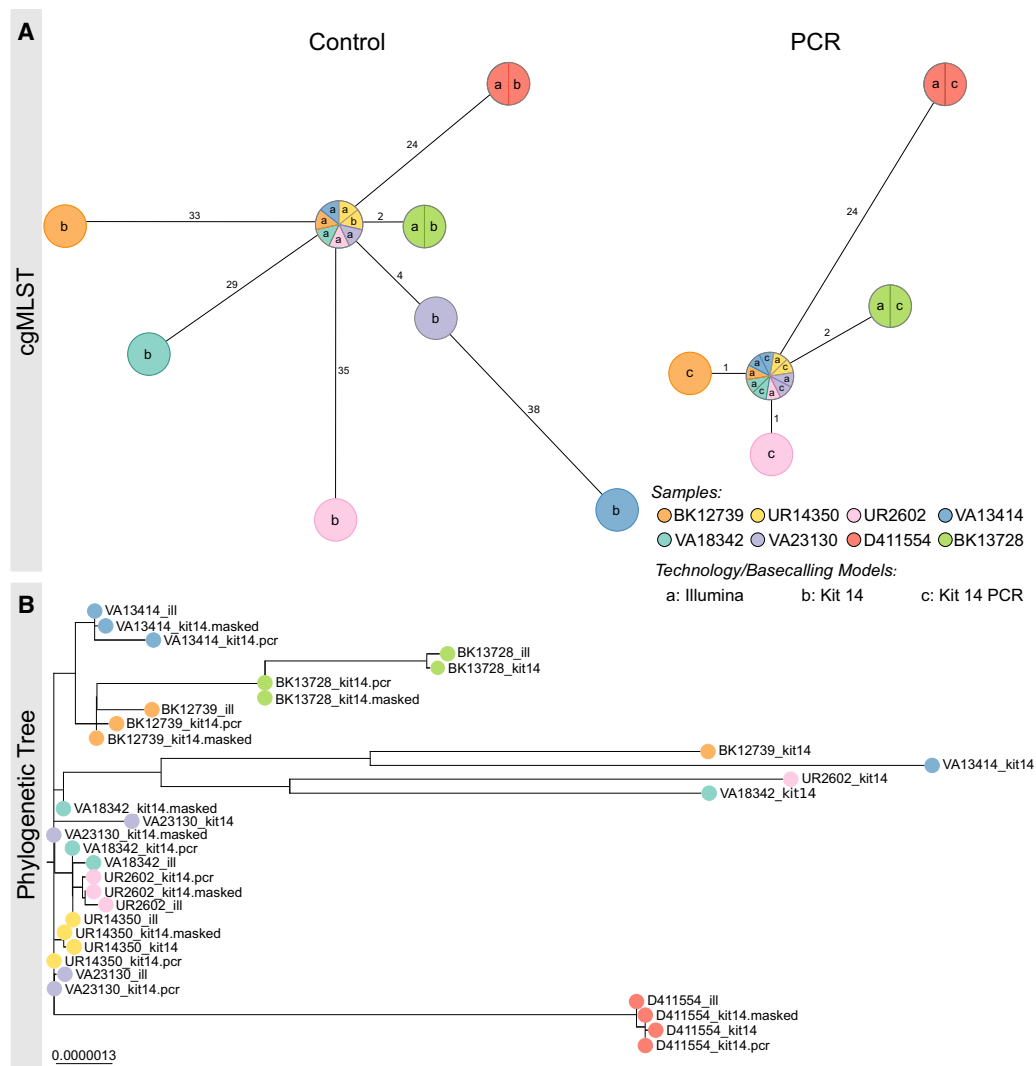


Figure 3. PCR-based sequencing or masking of ambiguous positions reduces allelic or phylogenetic distances. (A) Minimum spanning trees (pairwise ignore missing values) of each of eight *K. pneumoniae* outbreak samples based on 2358 genes to compare allelic differences between Illumina and Nanopore SQK-NBD114.24 genomes (Kit 14; left) and Illumina and Nanopore SQK-RPB114.24 genomes (PCR; right). Nodes (samples) are connected by lines depicting the distance by numbers of allelic differences. Loci are considered different whether one or more bases change between the samples. Loci without allelic differences are described as being the same. Samples with allelic differences of 15 or fewer are considered as part of the cluster. (B) Phylogenetic tree based on core genome SNP alignment between eight *K. pneumoniae* outbreak samples (colored nodes), prepared with Illumina (ill), Nanopore SQK-NBD114.24 (Kit 14), and SQK-RPB114.24 (Kit 14 PCR) compared with the masked Kit 14 assemblies (masked).

Based on our in-depth investigation, we recommend using the Nanopore rapid PCR barcoding kit for sequencing to eliminate these read ambiguities in the genome assemblies. However, this method decreases the read length to ~3500 bp, posing difficulties in achieving closed plasmids and genomes, similar to other short-read approaches but to a way lesser extent. A higher sequencing depth might also be necessary to control for polymerase errors. For samples already sequenced without any involvement of PCR, we propose using the provided MPOA workflow to assess the quality of each genome. This workflow offers information about the frequency and strand orientation of reads in ambiguous positions and masks them in the assembly by the IUPAC nucleotide code without needing another reference. These masked assemblies can be used for constructing phylogenetic trees for outbreak tracking. However, cgMLST cannot be performed as masked or degener-

ated bases create false allelic differences across the whole minimal spanning tree.

Given the notable strides made in direct methylation calling techniques, ONT might overcome the issues with ambiguous positions. If available in high enough quantities, duplex reads (connecting and sequencing both strands) might provide better raw signal data for accurate basecalling. The recently introduced research model reduces the ambiguous positions in direct comparison, but still a few remain (research model “res_dna_r10.4.1_e8.2_400bps_sup” available at GitHub (<https://github.com/nanoporetech/rerio>); not yet implemented in MinKNOW version 23.07.12, as of November 30, 2023) (Supplemental Table 4). Further advances that reduce methylation-induced errors for certain specific motifs are being developed, as shown for *Listeria monocytogenes* and *Escherichia coli* (Hallgren et al. 2021; Chiou et al. 2023).

Nevertheless, we strongly recommend constantly testing and evaluating reconstructed prokaryotic genomes to avoid erroneous conclusions based on these ambiguous positions introduced by unknown and not-yet-considered methylation motifs.

Methods

Isolates and genomic data

ONT sequencing data from three institutes have been collected and analyzed. The sequencing data include 264 isolates from 32 species, provided by the Leibniz-Institute of Photonic Technology Jena, Medical University of Graz, and University Hospital Jena. Additionally, a set of 80 samples containing *K. pneumoniae*, *E. faecalis*, *L. monocytogenes*, and *Staphylococcus aureus* from a ring trail were used for analysis (Dabernig-Heinz et al. 2024). University Hospital Leipzig provided 33 carbapenem-resistant *K. pneumoniae* outbreak isolates from sequence type 258 and the associated Illumina sequencing data (Supplemental Table 5). We ensured these samples were scattered across the whole phylogenetic tree that Viehweger et al. (2021) provided in their paper.

Genomic DNA isolation

Isolates from 10% glycerin cryo-culture were streaked out on Columbia agar with 5% sheep blood (Becton Dickinson). After overnight incubation, a single colony was selected and cultured overnight in MH-broth. Genomic DNA was isolated via ZymoBIOMICS DNA Microprep kit (ZymoResearch D4301 and D4305) with modifications to enhance the output yield. Qubit dsDNA BR assay-kit (Thermo Fisher Scientific) was employed to quantify DNA concentrations from each sample. This kit uses fluorescent dyes to measure double-stranded DNA to ensure reliable results.

Whole-genome sequencing

To prepare the library for sequencing using ONT's GridION system, we used the native barcoding kit 24 V12 (ONT SQK-NBD112.24) and native barcoding kit 24 V14 (ONT SQK-NBD114.24) with R10.4 and R10.4.1 flow cells, respectively. Both sequencing protocols were optimized regarding prolonged incubation times. Additionally, one library was prepared with rapid PCR barcoding kit 24 (ONT SQK-RPB114.24) for sequencing on an R10.4.1 flow cell. Sequencing of libraries prepared with SQK-NBD112.24 and SQK-NBD114.24 was conducted at 4 kHz with 260 bp, whereas SQK-RPB114.24 was conducted at 5 kHz with 400 bp. The DNA fragments minimum length for all sequencing runs was set to 200 bp in MinKNOW (v22.12.5) software.

Basecalling and assembly

Basecalling and barcode demultiplexing of long-read sequencing data were performed on the GridION (ONT) deploying Guppy (v6.4.6) using superaccurate models associated with the different used sequencing kits ("dna_r10.4_e8.1_sup.cfg," "dna_r10.4.1_e8.2_260bps_sup.cfg," "dna_r10.4.1_e8.2_5khz_400bps_sup.cfg"). For further analysis, Dorado (v0.3.0) was used ("dna_r10.4.1_e8.2_260bps_dna.cfg" and "dna_r10.4.1_e8.2_260bps_modbases_5mc_cg_sup.cfg").

Reads were filtered by excluding them below 1000 bp with Filtrong (v.0.2.1) (<https://github.com/rrwick/Filtrong>). De novo assembly was conducted using Flye (--meta --nano-hq; v2.9) (Kolmogorov et al. 2019). Filtered reads were mapped to the assembly using minimap2 (-ax map-ont; v2.18) (Li 2018) and polished afterward by Racon (v1.4.20; <https://github.com/lbcb-sci/racon>)

followed by medaka_consensus polishing both in default settings (v1.5.0; <https://github.com/nanoporetech/medaka>) using the following models: r104_e81_sup_g5015, dna_r10.4.1_e8.2_260bps_sup@v3.5.2, r1041_e82_260bps_sup_g632 (Supplemental Code 1). Short reads obtained by Illumina sequencing were assembled using Shovill (v1.1.0; <https://github.com/tseemann/shovill>), which includes various genome corrections and polishing approaches (Viehweger et al. 2021).

cgMLST of *K. pneumoniae*

For cgMLST, we used a species-specific public cgMLST scheme for a gene-by-gene comparison on an allelic level (Leopold et al. 2014; Mellmann et al. 2016) according to "*K. pneumoniae sensu lato* cgMLST" (<https://www.cgmlst.org/ncs/schema/2187931/>). This comprises a total of 2358 genes (~40% of the NTUH-K2044 reference genome) (Bialek-Davenet et al. 2014) in Flye-assembled and polished long-read and Shovill-assembled short-read assemblies (v1.1.0; github.com/tseemann/shovill). To illustrate the clonal relationships between different isolates, a minimum-spanning tree analysis was performed based on the determined allelic profiles using the Ridom SeqSphere+ software version 7 (Ridom) (Jünemann et al. 2013) with the parameter "pairwise ignore missing values." We defined a clonal transmission event if the isolates differ by 15 or more alleles for *K. pneumoniae* (Miro et al. 2020).

Phylogenetic tree

The phylogenetic trees visualize the evolutionary relationship among *K. pneumoniae* outbreak strains and are constructed based on core genome SNP alignment using Snippy-core (v4.6.0; github.com/tseemann/snippy). The phylogenetic tree was built using FastTree (Price et al. 2009) and visualized in Microreact (Argimón et al. 2016).

Workflow for detection and masking of ambiguous positions

We developed a standardized Nextflow (Di Tommaso et al. 2017) workflow for de novo quality validation of all species, which is publicly available at GitHub (<https://github.com/replikation/MPOA>), licensed under GNU general public license v3.0. The workflow only needs the genome file (FASTA) and the associated reads (FASTQ) (Fig. 4). The workflow provides reproducible quality control by counting and summarizing ambiguous bases for the user, masking low coverage regions (0x–10x depth) with BEDTools (v2.31.0) (Quinlan and Hall 2010), and providing an assembly with these positions masked by the IUPAC nucleotide code for subsequent analysis. The workflow utilizes Docker or singularity container and is compatible with a local run, Slurm, or Google Cloud Compute. Identification and masking of ambiguous positions were conducted using SAMtools consensus (v1.17) (Li et al. 2009) after minimap2 (v2.26; default) (Li 2018) or BWA (v0.7.17; alternative) mapping (Li and Durbin 2010). Different mapping approaches were tested (Supplemental Figs. 7, 8). PlasFlow (v1.1.0) (Krawczyk et al. 2018) extracts chromosome contigs for downstream analysis without plasmid sequences. R was utilized to plot sequence motifs (Fig. 2B) with ggseqlogo (Wagih 2017) and a violin chart comparing base frequencies per strand (Fig. 2A) with ggplot2 (Wickham 2016).

Data access

The ONT sequencing data generated in this study have been submitted to the NCBI BioProject database (<https://www.ncbi.nlm.nih.gov/bioproject/>) under accession number PRJNA1050168. The Illumina sequencing data used in this study have been

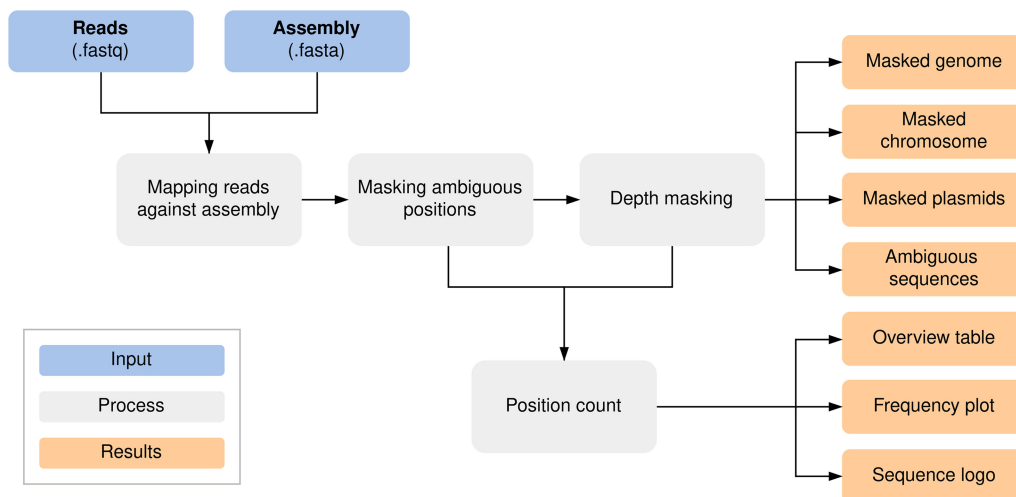


Figure 4. MPOA workflow to mask ambiguous and low coverage ($0\times$ – $10\times$ sequencing depth) positions in genome files. The workflow provides masked assemblies containing all contigs and separate masked chromosomes and plasmid FASTA files. A FASTA file per sample is also generated for each ambiguous position plus surrounding bases for further analysis (Supplemental Code 2; <https://github.com/replikation/MPOA>).

submitted to the NCBI BioProject database (<https://www.ncbi.nlm.nih.gov/bioproject/>) under accession number PRJNA742413. The workflow used in this study has been uploaded to GitHub (<https://github.com/replikation/MPOA>) and as Supplemental Code 2.

Competing interest statement

The authors declare no competing interests.

Acknowledgments

This work received financial support from the Ministry for Economics, Sciences and Digital Society of Thuringia (TMWWDG) under the framework of the Landesprogramm ProDigital (DigLeben-5575/10-9).

Author contributions: Sample collection and preparation were by M.L., A.V., and C.D. Sequencing was by M.L. Workflow development and testing were by M.L. and C.B. Bioinformatic analysis was by M.L. and C.B. Literature research was by M.L. Writing of the first draft was by M.L. Reviewing and editing the manuscript were by M.L., C.B., A.V., C.S., M.M., G.E.W., J.D.-H., R.E., S.D.B., S.M., C.D., and M.W.P. Supervision was by C.B. Project administration was by C.B. cgMLST analysis was by C.S. Funding acquisition was by C.B. Providing genomes was by M.L., S.D.B., S.M., A.V., G.E.W., and J.D.-H. All authors have read and agreed to the published version of the manuscript.

References

- Abe R, Oyama F, Akeda Y, Nozaki M, Hatachi T, Okamoto Y, Yoshida H, Hamaguchi S, Tomono K, Matsumoto Y, et al. 2021. Hospital-wide outbreaks of carbapenem-resistant Enterobacteriaceae horizontally spread through a clonal plasmid harbouring *bla*_{IMP-1} in children's hospitals in Japan. *J Antimicrob Chemother* **76**: 3314–3317. doi:10.1093/jac/dkab303
- Argimón S, Abudahab K, Goater RJE, Fedosejev A, Bhai J, Glasner C, Feil EJ, Holden MTG, Yeats CA, Grundmann H, et al. 2016. Microreact: visualizing and sharing data for genomic epidemiology and phylogeography. *Microb Genom* **2**: e000093. doi:10.1099/mgen.0.000093
- Bialek-Davenet S, Criscuolo A, Ailloud F, Passet V, Jones L, Delannoy-Vieillard A-S, Garin B, Le Hello S, Arlet G, Nicolas-Chanoine M-H, et al. 2014. Genomic definition of hypervirulent and multidrug-resistant *Klebsiella pneumoniae* clonal groups. *Emerg Infect Dis* **20**: 1812–1820. doi:10.3201/eid2011.140206
- Brandt C, Viehweger A, Singh A, Pletz MW, Wibberg D, Kalinowski J, Lerch S, Müller B, Makarewicz O. 2019. Assessing genetic diversity and similarity of 435 KPC-carrying plasmids. *Sci Rep* **9**: 11223. doi:10.1038/s41598-019-47758-5
- Brandt C, Krautwurst S, Spott R, Lohde M, Jundzill M, Marquet M, Hölzer M. 2021. poreCov—an easy to use, fast, and robust workflow for SARS-CoV-2 genome reconstruction via nanopore sequencing. *Front Genet* **12**: 711437. doi:10.3389/fgene.2021.711437
- Chewapreecha C, Holden MTG, Vehkala M, Välimäki N, Yang Z, Harris SR, Mather AE, Tuanyok A, De Smet B, Le Hello S, et al. 2017. Global and regional dissemination and evolution of *Burkholderia pseudomallei*. *Nat Microbiol* **2**: 16263. doi:10.1038/nmicrobiol.2016.263
- Chiou C-S, Chen B-H, Wang Y-W, Kuo N-T, Chang C-H, Huang Y-T. 2023. Correcting modification-mediated errors in nanopore sequencing by nucleotide demodification and reference-based correction. *Commun Biol* **6**: 1215. doi:10.1038/s42003-023-05605-4
- Dabernig-Heinz J, Lohde M, Hölzer M, Cabal A, Conzemius R, Brandt C, Kohl M, Halbedel S, Hyden P, Fischer MA, et al. 2024. A multicenter study on accuracy and reproducibility of nanopore sequencing-based genotyping of bacterial pathogens. *J Clin Microbiol* **62**: e00628-24. doi:10.1128/jcm.00628-24
- Di Tommaso P, Chatzou M, Floden EW, Barja PP, Palumbo E, Notredame C. 2017. Nextflow enables reproducible computational workflows. *Nat Biotechnol* **35**: 316–319. doi:10.1038/nbt.3820
- Dohm JC, Peters P, Stralis-Pavese N, Himmelbauer H. 2020. Benchmarking of long-read correction methods. *NAR Genom Bioinform* **2**: lqaa037. doi:10.1093/nargab/lqaa037
- Eid J, Fehr A, Gray J, Luong K, Lyle J, Otto G, Peluso P, Rank D, Baybayan P, Bettman B, et al. 2009. Real-time DNA sequencing from single polymerase molecules. *Science* **323**: 133–138. doi:10.1126/science.1162986
- Gao Q, Lu S, Wang Y, He L, Wang M, Jia R, Chen S, Zhu D, Liu M, Zhao X, et al. 2023. Bacterial DNA methyltransferase: a key to the epigenetic world with lessons learned from proteobacteria. *Front Microbiol* **14**: 1129437. doi:10.3389/fmicb.2023.1129437
- Grohme MA, Schloissnig S, Rozanski A, Pippel M, Young GR, Winkler S, Brandl H, Henry I, Dahl A, Powell S, et al. 2018. The genome of *Schmidtea mediterranea* and the evolution of core cellular mechanisms. *Nature* **554**: 56–61. doi:10.1038/nature25473
- Hadjadi L, Cassir N, Saidani N, Hoffman C, Brouqui P, Astoul P, Rolain J-M, Baron SA. 2022. Outbreak of carbapenem-resistant enterobacteria in a thoracic-oncology unit through clonal and plasmid-mediated transmission of the *bla*_{OXA-48} gene in southern France. *Front Cell Infect Microbiol* **12**: 1048516. doi:10.3389/fcimb.2022.1048516
- Hallgren MB, Overballe-Petersen S, Lund O, Hasman H, Clausen PTL. 2021. MINTyper: an outbreak-detection method for accurate and rapid SNP typing of clonal clusters with noisy long reads. *Biology Methods and Protocols* **6**: bpab008. doi:10.1093/biomethods/bpab008
- Jünemann S, Sedlazeck FJ, Prior K, Albersmeier A, John U, Kalinowski J, Mellmann A, Goesmann A, von Haeseler A, Stoye J, et al.

2013. Updating benchtop sequencing performance comparison. *Nat Biotechnol* **31**: 294–296. doi:10.1038/nbt.2522
- Kolmogorov M, Yuan J, Lin Y, Pevzner PA. 2019. Assembly of long, error-prone reads using repeat graphs. *Nat Biotechnol* **37**: 540–546. doi:10.1038/s41587-019-0072-8
- Krawczyk PS, Lipinski L, Dziembowski A. 2018. PlasFlow: predicting plasmid sequences in metagenomic data using genome signatures. *Nucleic Acids Res* **46**: e35. doi:10.1093/nar/gkx1321
- Leija-Salazar M, Sedlazeck FJ, Toffoli M, Mullin S, Mokretar K, Athanasopoulou M, Donald A, Sharma R, Hughes D, Schapira AHV, et al. 2019. Evaluation of the detection of *GBA* missense mutations and other variants using the Oxford Nanopore MinION. *Mol Genet Genomic Med* **7**: e564. doi:10.1002/mgg3.564
- Leopold SR, Goering RV, Witten A, Harmsen D, Mellmann A. 2014. Bacterial whole-genome sequencing revisited: portable, scalable, and standardized analysis for typing and detection of virulence and antibiotic resistance genes. *J Clin Microbiol* **52**: 2365–2370. doi:10.1128/JCM.00262-14
- Lerminiaux NA, Cameron ADS. 2019. Horizontal transfer of antibiotic resistance genes in clinical environments. *Can J Microbiol* **65**: 34–44. doi:10.1139/cjm-2018-0275
- Li H. 2018. Minimap2: pairwise alignment for nucleotide sequences. *Bioinformatics* **34**: 3094–3100. doi:10.1093/bioinformatics/bty191
- Li H, Durbin R. 2010. Fast and accurate long-read alignment with Burrows-Wheeler transform. *Bioinformatics* **26**: 589–595. doi:10.1093/bioinformatics/btp698
- Li H, Handsaker B, Wysoker A, Fennell T, Ruan J, Homer N, Marth G, Abecasis G, Durbin R, 1000 Genome Project Data Processing Subgroup. 2009. The Sequence Alignment/Map format and SAMtools. *Bioinformatics* **25**: 2078–2079. doi:10.1093/bioinformatics/btp352
- Linde J, Brangsch H, Hölzer M, Thomas C, Elschner MC, Melzer F, Tomaso H. 2023. Comparison of Illumina and Oxford Nanopore Technology for genome analysis of *Francisella tularensis*, *Bacillus anthracis*, and *Brucella suis*. *BMC Genomics* **24**: 258. doi:10.1186/s12864-023-09343-z
- Mellmann A, Bletz S, Böking T, Kipp F, Becker K, Schultes A, Prior K, Harmsen D. 2016. Real-time genome sequencing of resistant bacteria provides precision infection control in an institutional setting. *J Clin Microbiol* **54**: 2874–2881. doi:10.1128/JCM.00790-16
- Miro E, Rossen JWA, Chlebowicz MA, Harmsen D, Brisse S, Passet V, Navarro F, Friedrich AW, García-Cobos S. 2020. Core/whole genome multilocus sequence typing and core genome SNP-based typing of OXA-48-producing *Klebsiella pneumoniae* clinical isolates from Spain. *Front Microbiol* **10**: 2961. doi:10.3389/fmicb.2019.02961
- Moura de Sousa J, Lourenço M, Gordo I. 2023. Horizontal gene transfer among host-associated microbes. *Cell Host Microbe* **31**: 513–527. doi:10.1016/j.chom.2023.03.017
- Murray CJL, Ikuta KS, Sharara F, Swetschinski L, Robles Aguilar G, Gray A, Han C, Bisignano C, Rao P, Wool E, et al. 2022. Global burden of bacterial antimicrobial resistance in 2019: a systematic analysis. *Lancet* **399**: 629–655. doi:10.1016/S0140-6736(21)02724-0
- Ni Y, Liu X, Simeneh ZM, Yang M, Li R. 2023. Benchmarking of nanopore R10.4 and R9.4.1 flow cells in single-cell whole-genome amplification and whole-genome shotgun sequencing. *Comput Struct Biotechnol J* **21**: 2352–2364. doi:10.1016/j.csbj.2023.03.038
- Pletz MW, Wollny A, Dobermann U-H, Rödel J, Neubauer S, Stein C, Brandt C, Hartung A, Mellmann A, Trommer S, et al. 2018. A nosocomial food-borne outbreak of a VIM carbapenemase-expressing *Citrobacter freundii*. *Clin Infect Dis* **67**: 58–64. doi:10.1093/cid/ciy034
- Price MN, Dehal PS, Arkin AP. 2009. FastTree: computing large minimum evolution trees with profiles instead of a distance matrix. *Mol Biol Evol* **26**: 1641–1650. doi:10.1093/molbev/msp077
- Quinlan AR, Hall IM. 2010. BEDTools: a flexible suite of utilities for comparing genomic features. *Bioinformatics* **26**: 841–842. doi:10.1093/bioinformatics/btq033
- Sanderson ND, Kapel N, Rodger G, Webster H, Lipworth S, Street TL, Peto T, Crook D, Stoesser N. 2023. Comparison of R9.4.1/Kit10 and R10/Kit12 Oxford Nanopore flowcells and chemistries in bacterial genome reconstruction. *Microb Genom* **9**: mgen000910. doi:10.1099/mgen.0.000910
- Sivertsen A, Billström H, Melefos Ö, Liljequist BO, Wisell KT, Ullberg M, Özenci V, Sundsfjord A, Hegstad K. 2014. A multicentre hospital outbreak in Sweden caused by introduction of a *vanB2* transposon into a stably maintained pRUM-plasmid in an *Enterococcus faecium* ST192 clone. *PLoS One* **9**: e103274. doi:10.1371/journal.pone.0103274
- Spott R, Schleenvoigt BT, Edel B, Pletz MW, Brandt C. 2022. A rare case of periprosthetic streptobacillosis - rapid identification via nanopore sequencing after inconclusive VITEK MS results. *Arch Clin Med Case Rep* **6**: 613–617. doi:10.26502/acmcr.96550529
- Tourancheau A, Mead EA, Zhang X-S, Fang G. 2021. Discovering multiple types of DNA methylation from bacteria and microbiome using nanopore sequencing. *Nat Methods* **18**: 491–498. doi:10.1038/s41592-021-01109-3
- Tyson JR, O’Neil NJ, Jain M, Olsen HE, Hieter H, Snutch TP. 2018. MinION-based long-read sequencing and assembly extends the *Caenorhabditis elegans* reference genome. *Genome Res* **28**: 266–274. doi:10.1101/gr.221184.117
- Viehweger A, Blumenschein C, Lippmann N, Wyres KL, Brandt C, Hans JB, Hölzer M, Irber L, Gatermann S, Lübbert C, et al. 2021. Context-aware genomic surveillance reveals hidden transmission of a carbapenemase-producing *Klebsiella pneumoniae*. *Microb Genom* **7**: 000741. doi:10.1099/mgen.0.000741
- Wagh O. 2017. ggseqlogo: a versatile R package for drawing sequence logos. *Bioinformatics* **33**: 3645–3647. doi:10.1093/bioinformatics/btx469
- Wagner GE, Dabernig-Heinz J, Lipp M, Cabal A, Simantzik J, Kohl M, Scheiber M, Lichtenegger S, Ehrlich R, Leitner E, et al. 2023. Real-time nanopore Q20+ sequencing enables extremely fast and accurate core genome MLST typing and democratizes access to high-resolution bacterial pathogen surveillance. *J Clin Microbiol* **61**: e0163122. doi:10.1128/jcm.01631-22
- Wang Y, Zhao Y, Bollas A, Wang Y, Au KF. 2021. Nanopore sequencing technology, bioinformatics and applications. *Nat Biotechnol* **39**: 1348–1365. doi:10.1038/s41587-021-01108-x
- Wang X, Yu D, Chen L. 2023. Antimicrobial resistance and mechanisms of epigenetic regulation. *Front Cell Infect Microbiol* **13**: 1199646. doi:10.3389/fcimb.2023.1199646
- Wickham H. 2016. *ggplot2: elegant graphics for data analysis*. Springer-Verlag, New York.
- Wyres KL, Lam MMC, Holt KE. 2020. Population genomics of *Klebsiella pneumoniae*. *Nat Rev Microbiol* **18**: 344–359. doi:10.1038/s41579-019-0315-1

Received December 18, 2023; accepted in revised form May 7, 2024.